A Note on the Dipole Coordinates

Akira Kageyama,* Tooru Sugiyama, Kunihiko Watanabe, and Tetsuya Sato

Earth Simulator Center, Japan Agency for Marine-Earth Science and Technology, Yokohama 236-0001, Japan

A couple of orthogonal coordinates for dipole geometry are proposed for numerical simulations of plasma geophysics in the Earth's dipole magnetic field. These coordinates have proper metric profiles along field lines in contrast to the standard dipole coordinate system that is commonly used in analytical studies for dipole geometry.

I. INTRODUCTION

In the study of plasma geophysics, an orthogonal coordinate system defined by a dipole field is commonly used because of the Earth's dipole magnetic field $\mathbf{B}_d$. The standard dipole coordinate system (μ, χ, ϕ) is defined through the spherical coordinates (r, θ, ϕ) as

$$\mu = -\frac{\cos \theta}{r^2}, \qquad \chi = \frac{\sin^2 \theta}{r}, \tag{1}$$

where r is length from Earth's center, normalized by its radius $1Re$, θ is colatitude, and ϕ is the longitude. The coordinate μ is a potential function of a dipole field, $\mathbf{B}_d \propto \nabla \mu$, and constant–$\chi$ curves in a meridian plane, $\phi = \text{const.}$, denote dipole filed lines.

Since (μ, χ, ϕ) is an orthogonal system, their metric terms are simply given by

$$h_\mu = 1 / |\nabla \mu| = r^3 / \Theta, \tag{2}$$
$$h_\chi = 1 / |\nabla \chi| = r^2 / (\Theta \sin \theta), \tag{3}$$
$$h_\phi = 1 / |\nabla \phi| = r \sin \theta, \tag{4}$$

with

$$\Theta(\theta) = \sqrt{1 + 3 \cos^2 \theta}, \tag{5}$$

and the length element ds is given by $ds^2 = ds_\mu^2 + ds_\chi^2 + ds_\phi^2$ with $ds_\mu = h_\mu \, d\mu$, $ds_\chi = h_\chi \, d\chi$, $ds_\phi = h_\phi \, d\phi$. Given these metric terms, it is straightforward to discretize any differential operator such as the divergence of a vector $\mathbf{v}$ that is denoted by components $\{v_\mu, v_\chi, v_\phi\}$ in the dipole coordinates as

$$\nabla \cdot \mathbf{v} = \frac{1}{h_\mu h_\chi h_\phi} \frac{\partial}{\partial \mu}(h_\chi h_\phi v_\mu) + \frac{1}{h_\mu h_\chi h_\phi} \frac{\partial}{\partial \chi}(h_\phi h_\mu v_\chi) + \frac{1}{h_\mu h_\chi h_\phi} \frac{\partial}{\partial \phi}(h_\mu h_\chi v_\phi), \tag{6}$$

by, for example, a finite difference method in the computational (μ, χ, ϕ) space.

The above standard dipole coordinates is convenient and certainly appropriate for analytical studies in which the Earth's dipolar field plays central roles. It also works as a base coordinates for the node and cell generation of the finite element method in the dipole geometry [2, 3]. However, when one tries to use other numerical methods in which analytical expression of the metric terms are important for preserving numerical simplicity and accuracy, as in the case of the finite difference method, the standard dipole coordinate (μ, χ, ϕ) cannot be used in its original form since the metric h_μ changes intensely along the field lines.

It should be noted that $h_\mu \propto |\mathbf{B}_d|^{-1}$ from the above definitions, which means that h_μ is roughly proportional to r^3. Therefore, the metric h_μ at $r = 1$ is $O(10^3)$ smaller than that at $r = 10$. Fig. 1(a) shows the h_μ profile along a field line starting from 70°N as a function of μ. (We suppose that the north pole is located in $\theta = 0$ in this note.) This field line goes through the equator ($\mu = 0$) at $r = 8.55$. Note the sharp peak in Fig. 1(a) at the equator.

When one uses the finite central difference method, the grid spacing along the field line is given by $\Delta s_\mu = h_\mu \Delta \mu$. Fig. 2 shows grid point distribution in the standard dipole coordinates. The grid size in the figure is $N_\mu \times N_\chi = 101 \times 10$. (101 grids along each field line and 10 grids in the perpendicular direction.) The starting points of the field lines are

*Electronic address: kage@jamstec.go.jp

between 65°N and 70°N at $r = 1$. All the grid points are shown in the figure without any skip. It is clearly seen that the resolution near the equator is so poor that any numerical simulation on this grid system is impractical. For the field line starting from 70°N at $r = 1$, the metric h_μ on the equator is about 1160 times larger than that on $r = 1$. Also note that the imbalance of the grid spacings between the near Earth and the near equatorial regions along the field lines causes unnecessarily severe restriction on the Courant-Friedrichs-Lewy condition in explicit time integration schemes.

For some numerical simulations such as the magnetosphere-ionosphere coupling, it is certainly desirable to use a grid system that has a natural grid convergence near the ionosphere to resolve fine structures near the coupling region, but the three-orders of magnitude is obviously too much. This is especially serious when one tries to simulate some phenomena in which relatively high resolution near the equator is required. An example of such simulation is the auroral arc formation by the feedback instability driven by vortex flow in the equator [11, 12].

A trivial way to avoid the poor resolution problem of the standard dipole coordinates near the equator is to place the computational grid points along the μ space in a nonuniform way. In this case, the metric factors have to be numerically calculated. For example, Lee and Lysak [6, 7] determined the grid spacing due to the local Alfvén wave speed. The same approach was adopted in Budnik et al. [1]. However, this method injures the generality of the dipole coordinates as well as its analytical nature.

If one prefers to fully numerical methods, refer to Proehl et al. [9] in which a general algorithm to construct grid points along an arbitrarily given magnetic field, including the dipole, is presented. In contrast to that approach, we propose in this note analytical as well as simple coordinate transformations of μ that lead to practical metric distributions along the field line.

II. TRANSFORMATION FORMULA OF THE DIPOLE COORDINATES

Before we go into the description on the modified dipole coordinates defined by the coordinate transformation of the standard dipole coordinates, we derive analytical expressions of the inverse transformation from the standard dipole coordinates (μ, χ, ϕ) into the spherical coordinates (r, θ, ϕ) since we could not find these expressions in the literature and they can be directly applied to the modified dipole coordinates described later.

Eliminating r from in eq. (1) with subsidiary variables u and ζ defined as

$$u = \sin^2 \theta, \quad \zeta = (\mu/\chi^2)^2, \tag{7}$$

we get a fourth order equation of u:

$$\zeta u^4 + u - 1 = 0. \tag{8}$$

The unique solution of eq. (8) for positive real u is

$$u = -\frac{1}{2}\sqrt{w} + \frac{1}{2}\sqrt{-w + \frac{2}{\zeta\sqrt{w}}}, \tag{9}$$

where

$$w(\zeta) = -\frac{c_1}{\gamma(\zeta)} + \frac{\gamma(\zeta)}{c_2\,\zeta}, \tag{10}$$

$$c_1 = 2^{7/3}\,3^{-1/3}, \quad c_2 = 2^{1/3}\,3^{2/3}, \tag{11}$$

and

$$\gamma(\zeta) = \left(9\,\zeta + \sqrt{3}\,\sqrt{27\,\zeta^2 + 256\,\zeta^3}\right)^{1/3}. \tag{12}$$

The analytical expression for r and θ by μ and χ are, therefore, given by the function u:

$$r(\mu, \chi) = u\,/\,\chi, \tag{13}$$

$$\theta(\mu, \chi) = \arcsin\sqrt{u}, \tag{14}$$

where arcsin is defined as a continuous function of u with the range of $[0, \pi]$.

III.   MODIFIED DIPOLE COORDINATES

The problem of the metric imbalance along field lines in the standard dipole coordinates originates from the power 2 of the μ's denominator r^2 in eq. (1). Therefore, one simple idea to reduce the steep metric distribution in the standard dipole coordinates shown in Fig. 1(a) is to use a coordinates (μ', χ, ϕ) in which field-aligned coordinate μ', instead of μ, is defined as

$$\mu' = -\frac{\sqrt{\cos\theta}}{r}, \qquad \text{for} \quad \theta < \pi/2. \tag{15}$$

It is easy to confirm that (μ', χ, ϕ) is also an orthogonal system. The metric of μ'-coordinate is given by

$$h_{\mu'} = 1 / |\nabla\mu'| = 2\, r^2 \sqrt{\cos\theta} / \Theta. \tag{16}$$

Hysell et al. [4] used essentially the same coordinates as (μ', χ, ϕ) for a plasma clouds simulation in midlatitude. (They used $M \equiv r/\sqrt{\cos\theta} = -1/\mu'$, instead of μ'.) When one uses this coordinate system (μ', χ, ϕ), a care should be taken for the fact that the metric $h_{\mu'}$ vanishes in the equator; $h_{\mu'}|_{\mu'=0} = 0$. This was not a problem in the simulation by Hysell et al. [4] since it was sufficient for them to use only a small part of the μ' space ($-0.79 \leq \mu' \leq -0.74$).

A simple remedy to avoid the singularity of $h_{\mu'}$ in the equator is not to place the grid point just on the equator. For example, the northern hemisphere is fully covered in practice by $\mu' \leq 0 - \epsilon_{\mu'}$, or $\theta \leq \pi/2 - \epsilon_\theta$, with a small positive buffer $\epsilon_{\mu'}$ or ϵ_θ. Fig. 3 shows the grid points with $N_{\mu'} \times N_\chi = 51 \times 10$ for the practically full range of the northern hemisphere by setting $\epsilon_\theta = 0.01$.

The transformation formula for the modified dipole coordinates (μ', χ, ϕ) into the spherical coordinates are obtained by the same equation (8) by letting $\zeta = (\mu'/\chi)^4$.

Another form of modified orthogonal dipole coordinates proposed in this note is (ψ, χ, ϕ), where the new coordinate ψ is defined through μ as

$$\psi = \sinh^{-1}(a\,\mu) / \bar{a}, \tag{17}$$

or its inverse transformation

$$\mu = \sinh(\bar{a}\,\psi) / a, \tag{18}$$

where a is a parameter that controls the grid distribution along dipole field lines, and $\bar{a}$ is defined as $\bar{a} = \sinh^{-1} a$. Note the identity of $\sinh^{-1} x = \log\left(x + \sqrt{1 + x^2}\right)$.

The metric of ψ is given by

$$h_\psi = h_\mu \frac{d\mu}{d\psi} = \bar{a}\, r^3 \cosh(\bar{a}\,\psi) / (a\,\Theta). \tag{19}$$

The h_ψ distribution as a function of ψ when the control parameter $a = 100$ is shown in Fig. 1(b), which should be compared with h_μ distribution shown in Fig. 1(a). It should be noted that the vertical scales in Fig. 1(a) and (b) are different for one order of magnitude. The basic idea that has lead to the transformation (17) is to relax the steep gradient of the metric along μ in Fig. 1(a) by local scale transformations. We want to make the μ grid spacing along the field line being "shrunk" only near the equator; $\mu \sim 0$ or $\psi \sim 0$. Therefore, the grid "shrink rate" along the field line should be a function with a steeple-like peak at $\psi = 0$. An example of such a function is $1/\cosh\psi$. The grid shrink rate is given by $d\psi/d\mu$ since it is the reciprocal of the grid "stretch rate" $d\mu/d\psi$; see eq. (19). Solving $d\psi/d\mu = 1/\cosh\psi$, we get $\mu = \sinh\psi$.

In the limit of $a \to 0$, $\psi = \mu$. As the parameter a increases, grid points near the Earth ($r = 1$) along field lines, which are highly concentrated in the standard dipole coordinates (see the upper panel of Fig. 2), move toward the equator along the field lines. The denominator $\bar{a}$ in eq. (17) is introduced to keep the transformed coordinate ψ being always in the range of $[-1, 1]$. Fig. 4 shows grid points distribution when $a = 100$ for $N_\psi \times N_\chi = 101 \times 10$. The metric h_ψ for the field line starting from 70°N on the equator is only 12 times larger than that on $r = 1$. The coordinate transformation by the sinh-function—applied to the cartesian coordinates—was also used in our numerical simulations of the magnetosphere [5, 10].

The coordinates transformations from (ψ, χ, ϕ) into (r, θ, ϕ) are given by eqs. (13) and (14) with eq. (18).

The relation between components of a vector $\mathbf{v}$ in the spherical coordinates $\{v_r, v_\theta, v_\phi\}$ and in the modified dipole coordinates $\{v_\psi, v_\chi, v_\phi\}$ is given by the same form as that in the standard dipole coordinates:

$$\begin{pmatrix} v_\psi \\ v_\chi \\ v_\phi \end{pmatrix} = \begin{pmatrix} 2\cos\theta/\Theta & \sin\theta/\Theta & 0 \\ -\sin\theta/\Theta & 2\cos\theta/\Theta & 0 \\ 0 & 0 & 1 \end{pmatrix} \begin{pmatrix} v_r \\ v_\theta \\ v_\phi \end{pmatrix}. \tag{20}$$

The inverse transformation is given by the transverse matrix.

IV. DISCUSSION AND SUMMARY

The standard dipole coordinates (μ, χ, ϕ) defined by eq. (1) is not a good choice for a base grid in numerical studies since the metric contrast along each field line is too intense. Instead of the standard dipole coordinates, we propose to use the modified orthogonal dipole coordinates defined by

$$(\psi, \chi, \phi) = \left(-\frac{\sinh^{-1}\left(a\cos\theta/r^2\right)}{\sinh^{-1} a}, \frac{\sin^2\theta}{r}, \phi \right),\tag{21}$$

with a tuning parameter a of the metric distribution along field lines. The standard dipole coordinates is a special case in the limit of $a \to 0$. Fig. 4 shows the case when $a = 100$ for the field lines with foot points located between 65°N and 70°N. Since ψ's metric, or the grid distribution, is not sensitive to the change of a around this value, one would not have to perform its fine control. For other χ range, pertinent a value will be easily found by visual checks of grid distribution images like Fig. 4.

For problems in which a symmetry around the equator between the northern and southern hemispheres is present, one can also try another form of modified orthogonal dipole coordinates defined by

$$(\mu', \chi, \phi) = \left(-\frac{\sqrt{\cos\theta}}{r}, \frac{\sin^2\theta}{r}, \phi \right),\tag{22}$$

in which $\mu' \leq 0 - \epsilon$, with a small positive buffer ϵ for the northern hemisphere.

Recently, a non-orthogonal dipole coordinates that is designed so that the lower-most constant-μ surface coincides with a constant-r surface (i.e., a sphere) is presented [8]. It is straightforward and effective to apply the coordinate transformations presented in this note for that nonorthogonal dipole coordinates, too.

---

[1] Budnik, F., Stellmacher, M., Glassmeier, K.-H., and Buchert, S. C. (1998). Ionospheric conductance distribution and MHD wave structure: observation and model. *Annales Geophysicae*, 16:140–147.

[2] Fujita, S., Itonaga, M., and Nakata, H. (2000). Relationship between the Pi2 pulsations and the localized impulsive current associated with the current disruption in the magnetosphere. *Earth, Planets and Space*, 52:267–281.

[3] Fujita, S., Nakata, H., Itonaga, M., Yoshikawa, A., and Mizuta, T. (2002). A numerical simulation of Pi2 pulsation associated with the substorm current wedge. *Journal of Geophysical Research*, 107(A3).

[4] Hysell, D. L., Chau, J. L., and Fesen, C. G. (2002). Effects of large horizontal winds on the equatorial electrojet. *Journal of Geophysical Research*, 107.

[5] Kageyama, A., Watanabe, K., and Sato, T. (1992). Global simulation of the magnetosphere with a long tail: No interplanetary magnetic field. *Journal of Geophysical Research*, 97(A4):3929–3943.

[6] Lee, D.-H. and Lysak, R. L. (1989). Magnetospheric ULF wave coupling in the dipole model: the impulsive excitation. *Journal of Geophysical Research*, 94(A12):17097–17103.

[7] Lee, D.-H. and Lysak, R. L. (1991). Impulsive excitation of ULF waves in the three-dimensional dipole model: The initial results. *Journal of Geophysical Research*, 96(A3):3479–3486.

[8] Lysak, R. L. (2004). Magnetosphere-ionosphere coupling by Alfvén waves at midlatitudes. *Journal of Geophysical Research*, 109.

[9] Proehl, J. A., Lotko, W., Kouznetsov, I., and Geimer, S. D. (2002). Ultralow-frequency magnetohydrodynamics in boundary-constrained geomagnetic flux coordinates. *Journal of Geophysical Research*, 107(A9).

[10] Usadi, A., Kageyama, A., Watanabe, K., and Sato, T. (1993). A global simulation of the magnetosphere with a long tail: Southward and northward interplanetary magnetic field. *Journal of Geophysical Research*, 98(A5):7503–7518.

[11] Watanabe, K. and Sato, T. (1988). Self-excitation of auroral arcs in a three-dimensionally coupled magnetosphere-ionosphere system. *Geophysical Research Letters*, 15:717–720.

[12] Watanabe, T., Oya, H., Watanabe, K., and Sato, T. (1993). Comprehensive simulation study on local and global development of auroral arcs and field-aligned potentials. *Journal of Geophysical Research*, 98:21391–21407.
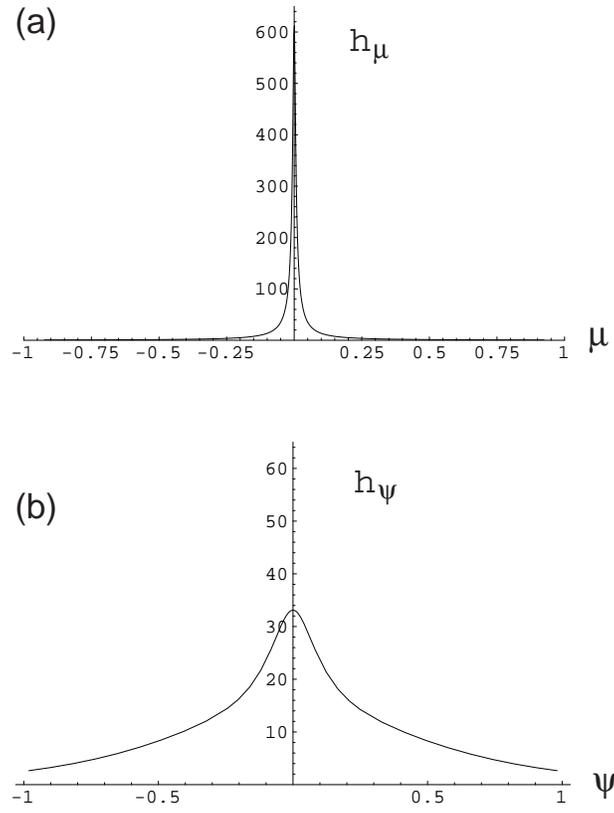
FIG. 1: The metric distribution along field the line starting from $70°$N at $r = 1$. (a) h_μ for the standard dipole coordinates (b) h_ψ for the modified dipole coordinates. Note that the vertical scales between the two panels (a) and (b) are different for one order of magnitude.

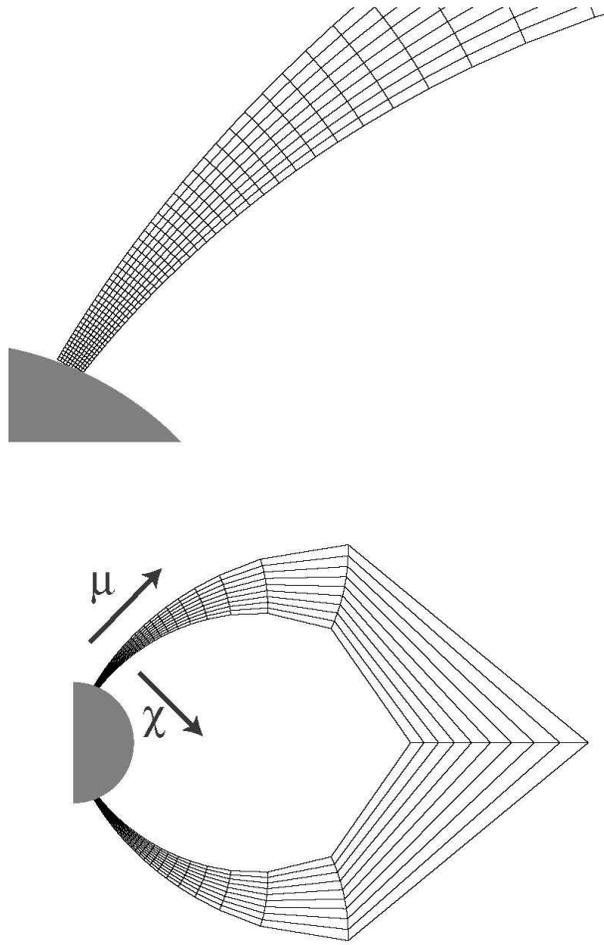FIG. 2: The standard dipole coordinates $(\mu, \chi, \phi) = (-\cos\theta \,/\, r^2, \sin^2\theta \,/\, r, \phi)$ in a meridian plane, $\phi = $ const. The grid points are distributed with equal spacings in each direction in the computational space μ and χ. The total grid size is $N_\mu \times N_\chi = 101 \times 10$. There is no skip of grid points in the figure. The starting points of the field lines are between $65°$N and $70°$N at $r = 1$. The upper panel is a closer view.
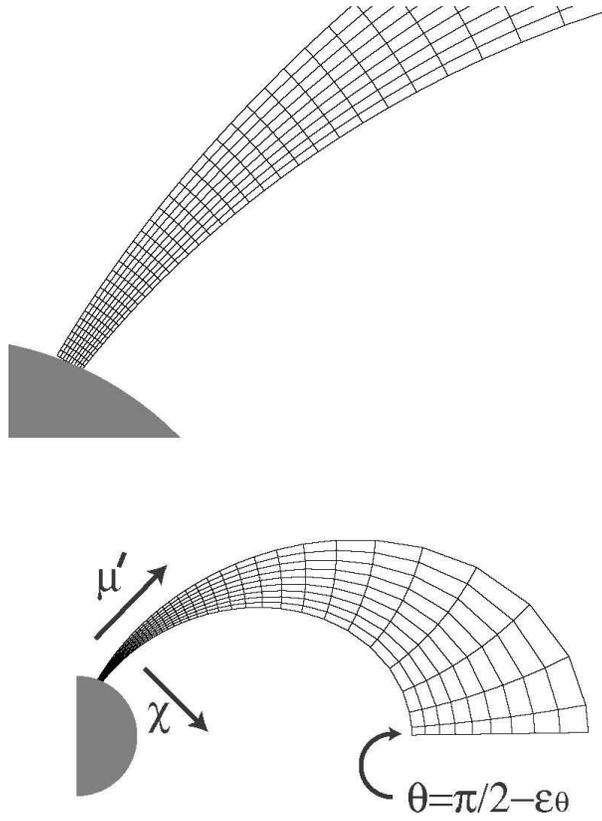
FIG. 3: Modified orthogonal dipole coordinates (μ', χ, ϕ) in a meridian plane. The coordinate μ' is defined as $\mu' = -\sqrt{\cos\theta}\,/\,r$, with $\mu' \leq 0 - \epsilon_{\mu'}$, or $\theta \leq \pi/2 - \epsilon_\theta$. The small buffer $\epsilon_{\mu'}$ or ϵ_θ is introduced to avoid the vanishing metric in the equator. ($h_{\mu'} = 0$ at $\mu' = 0$.) Here $\epsilon_\theta = 0.01$. The total grid size is $N_{\mu'} \times N_\chi = 51 \times 10$ in this "almost" northern hemispheric region.
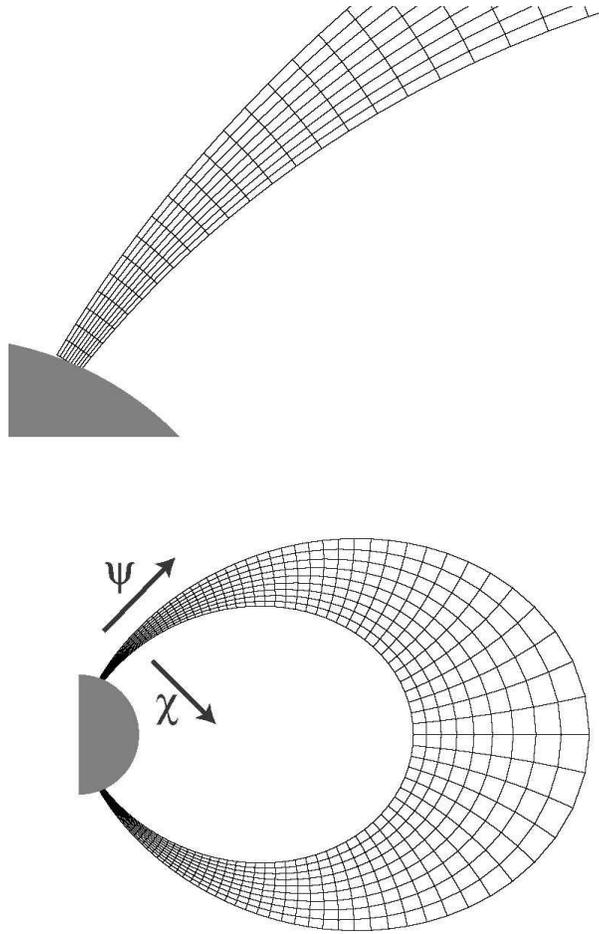
FIG. 4: Modified orthogonal dipole coordinates (ψ, χ, ϕ) in a meridian plane. The coordinate ψ is defined as $\psi = \sinh^{-1}(a\,\mu)\,/\,\sinh^{-1}a$. Total grid size is $N_\psi \times N_\chi = 101 \times 10$. The control parameter $a = 100$ in this figure. Compare with the grid distribution of the standard dipole coordinates (Fig. 2) with the same grid size.